This is the Pre-Published Version.
S. Lin, X. Huang, J. Gao, J. Ji (2021) *Extinction of Wood Fire: A Near-Limit Blue Flame above Hot Smoldering Surface*, **Fire Technology**. https://doi.org/10.1007/s10694-021-01146-6

Extinction of Wood Fire: A Near-Limit Blue Flame above Hot Smoldering Surface

Shaorun Lin[1,2], Xinyan Huang[1,*], Jian Gao[3,*], Jie Ji[4]

[1]*Research Centre for Fire Safety Engineering, The Hong Kong Polytechnic University, Hong Kong*
[2]*The Hong Kong Polytechnic University Shenzhen Research Institute, Shenzhen, China*
[3]*Qingdao Institute of Bioenergy and Bioprocess Technology, Chinese Academy of Sciences, Qingdao, China*
[4]*State Key Laboratory of Fire Science, University of Science and Technology of China, Hefei, China*
* Corresponding to xy.huang@polyu.edu.hk; gaojian@qibebt.ac.cn;

Abstract: Timber is cost-effective and environmentally-friendly, which is a potential material for sustainable buildings, but its fire safety is still a significant concern. In this work, we investigate the burning behaviors of different types of woods and their self-extinction mechanism under external radiation. A unique near-limit flame is observed when the irradiation is above a critical value of about 40 kW/m^2. Such a near-limit flame is weak, blue, and discrete that tends to attach to the wood residue surface, different from the normal buoyancy-controlled sooty yellow flame. If the irradiation is low (<40 kW/m^2), the yellow flame extinguishes and transits directly to smoldering at the mass flux of about 4 g/m^2·s. However, above the critical irradiation level, the yellow flame transits to the blue flame that does not extinguish until the mass flux of around 1 g/m^2·s, extending the flame extinction limit of timber materials. The near-limit blue flame may appear only if the char surface temperature exceeds 700 ℃. Two critical conditions are hypothesized for this unique blue flame, (I) in-depth pyrolysis (mainly lignin) sustained by the internal smoldering combustion, and (II) the hot surface maintained by large external radiation to extend the flammability limit. This unique blue flame may play an essential role in the transition between flaming and smoldering and help evaluate the fire risk of timber materials under real fire scenarios.

Keywords: extinction limit; external radiation; flaming-to-smoldering transition; timber fire.

Graphic Abstract:

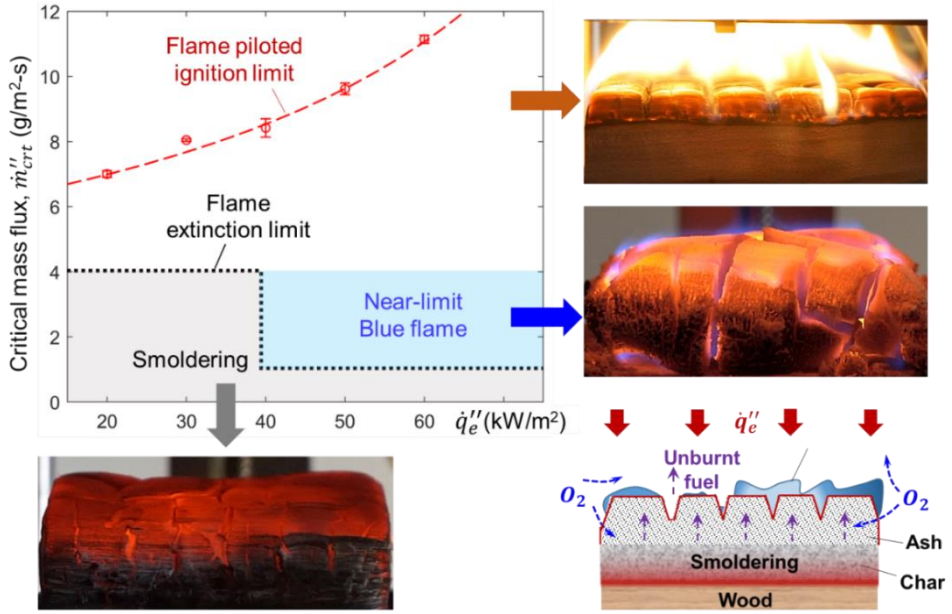

1. Introduction

Timber, as a renewable and sustainable material, is reconsidered as a preferred construction material for high-rise buildings owing to its abundance in nature, high stiffness, and the high strength-to-weight ratio [1–3]. In recent years, many environmental-friendly high-rise timber buildings have sprung up rapidly all around the world, e.g., the 18-story timber building (85 m) in Brumunddal, Norway (Fig. 1a). Attributed to innovative timber materials like the cross-laminated timber (CLT) [4,5], Sumitomo made a plan to build a 70-story (350 m) timber skyscraper in Tokyo by 2041 [6]. However, the fire risk of timber is still the primary concern, and the application of high-rise timber building is highly controversial [1,3], because of its flammable nature and large fuel load in structures [7]. For example, a recent fire in Notre Dame Cathedral (Fig. 1b) burnt out its wooden frame that was made of oak about 800 years ago [8]. Thus, it is urgent to fully understand the fire dynamics and combustion limits of timber materials with the fast growing of timber buildings [2,9].

In the literature, the ignition of various timbers or wooden materials has been studied extensively to understand the initiation and growth of timber fires [10–16]. Like most flammable materials, the combustion limits and fire behaviors of timber materials can be influenced by both environmental (*e.g.*, heating source, oxygen concentration, and wind velocity) and material (*e.g.*, density, composition, moisture, and age) factors [17–21]. Moreover, timber, as a typical charring material, can sustain both flaming and smoldering combustion [13]. Flaming is a gas-phase combustion process, while smoldering is the slow, low-temperature, and flameless burning of porous fuels and is the most persistent type of combustion phenomenon [22]. For high-density wood fuels, the difficulty of ignition in terms of the ignition delay time under the external irradiation is found to increase from the piloted flaming ignition to flaming autoignition, and to smoldering (or glowing/surface) ignition [23–25]. This is different from low-density and high-porosity materials (e.g., PU foam and peat soil), for which smoldering ignition is the easiest [22,25].

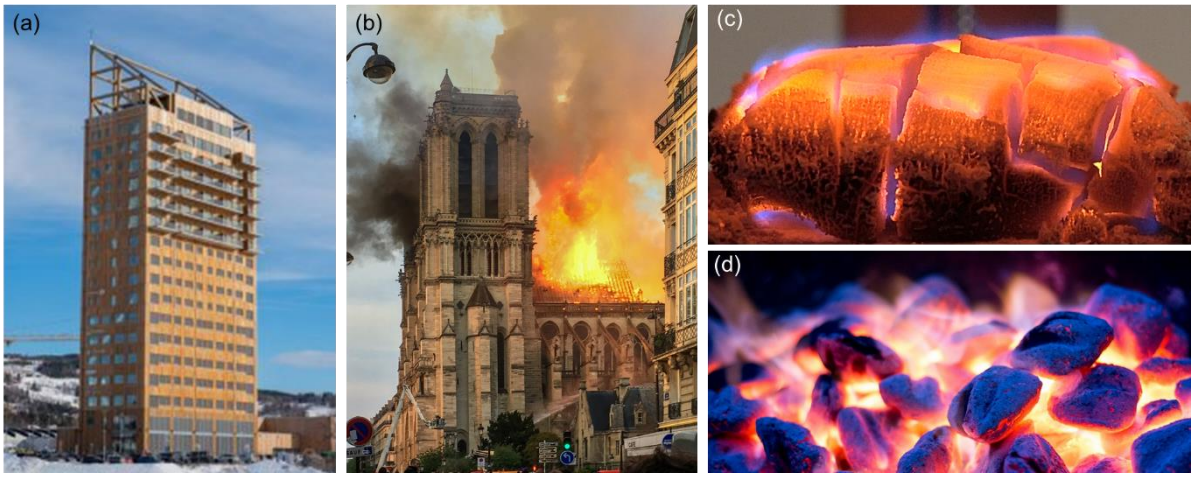

Fig. 1. (a) The 18-story apartment building Mjøstårnet in Norway (Photo courtesy the Council on Tall Buildings and Urban Habitat), (b) the Notre-Dame de Paris fire on 15 April 2019 (Photo courtesy Wiki Commons), and the blue flame above the (c) timber (cc by S. Lin), and (d) charcoal (cc by M. Simon).

On the other hand, a flame is sometimes found not to be able to sustain above the timber material after ignition, i.e., the self-extinction may occur [10,26,27]. The self-extinction of timber flame is a crucial concept that supports the fire safety of high-rise timber building and its fast-growing market [9,26,28,29]. However, very few studies have investigated the extinction mechanisms of timber and quantified its combustion limits. Previously, Babrauskas [30] used a flame to ignite a timber material for several minutes and found the self-extinction occurred once the igniting flame was removed. Emberley *et al.* [9,15] further studied the self-extinction of flaming timber and CLT under external radiation and found the critical heat flux of 43.6 ± 4.7 kW/m^2 and the minimum mass flux of 3.93 ± 0.45 g/m^2·s were required to sustain the flame. Vermesi *et al.* [17] found that for engineered wood, the critical mass flux for flameout varied in a wide range (1.4-17 g/m^2·s). Nevertheless, extinction of the flame is not the end of a fire, as it may be followed by the smoldering [31]. Moreover, under specific conditions, smoldering may also transition back to the flaming, i.e., the smoldering-to-flaming (StF) transition [22,32]. Therefore, in a real timber fire, the ignition (and re-ignition) and extinction of the flame, as well as smoldering combustion, could repeatedly occur several times until the eventual burnout, during which the timber material loses its stability or even collapses [15].

In our recent wood fire tests, a thin layer of weak blue flame (Fig. 1c) was observed floating above the wood surface near the flaming extinction limit. A similar blue flame is also widely observed in the burning charcoal (Fig. 1d). Such a near-limit blue flame may play an important role in defining the true extinction limit of timber flame and the transition between flaming and smoldering, while to the best of authors' knowledge, the combustion mechanism dominating this unique phenomenon has not been systematically studied yet, posing a knowledge gap. In this work, we will quantify the extinction limits of timber flame and its near extinction fire behaviors using both laboratory experiments and phenomenological analysis.

2. Experimental methods

Six different types (species) of natural woods, which have the same dimension of 10 cm × 10 cm × 3 cm and different densities, were tested (Fig. 2a). Before the experiments, all wood samples were first oven-dried at 70 ℃ for 48 h, and then, placed into an electronic dry cabinet to avoid the re-absorption of moisture from the air. Their dry bulk densities from low to high are listed in Table 1. The thermal analysis for all wood samples was conducted with a PerkinElmer STA 6000 Simultaneous Thermal Analyzer in both air and nitrogen flows, and the representative data are shown in Appendix (Fig. A1).

All experiments were conducted under the cone calorimeter (FTT iCone Plus), which mainly includes a conical heater, spark igniter, sample holder, and precision scale, as illustrated in Fig. 2(b). The conical heater could provide relatively constant and uniform irradiation ($\dot{q}_e''$) to the sample area of 10 cm ×10 cm, so that the whole top surface of the wood sample would have uniform irradiation [33]. Before the test, the temperature of the conical heater was calibrated with the irradiation level,

which was measured by a radiometer. The test section, including the wood sample, sample holder, and cone heater, was partially open to ensure a sufficient air supply and smoke ventilation.

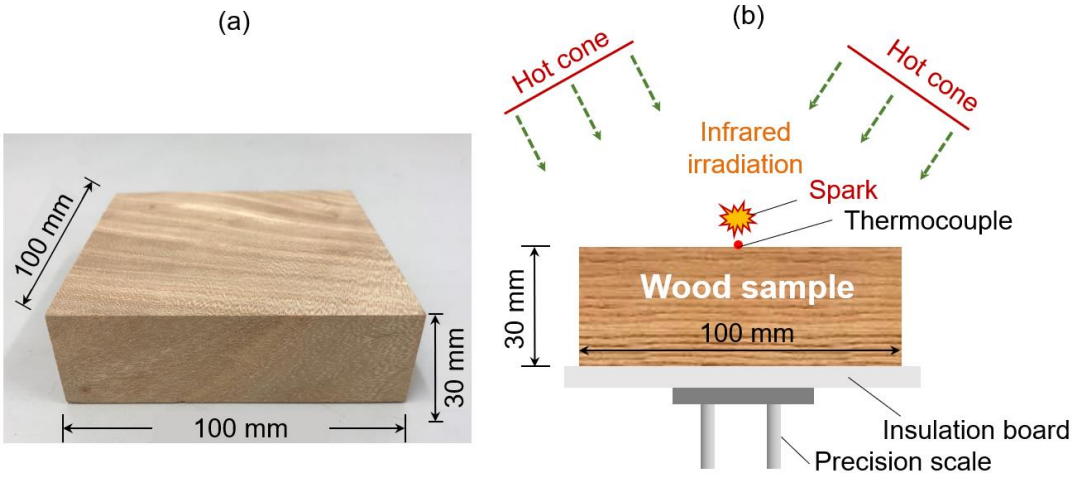

Fig. 2. (a) A photo of the wood sample, and (b) a schematic diagram of the experimental apparatus.

The piloting spark was placed at 5 mm above the top surface of the wood sample. Once the flame was piloted, the spark was removed, while heating was continued until the sample mass no longer changed or the wood sample completely turned into white ashes (i.e., burnout). The test process was recorded by a side-view camera, and the sample mass was monitored by the precision scale (± 0.1 mg). The surface temperature of wood was carefully monitored using a K-type thermocouple (0.5 mm junction bead diameter) that was contacted with the wood top surface. During the test, the ambient temperature was 22 ± 2 ℃, the relative humidity was 50 ± 10%, and the ambient pressure was 1 atm. For each test, at least two repeating experiments were conducted to ensure the experimental repeatability and quantify the experimental random uncertainty, which is shown as error bars in plots.

Table 1. The dry bulk density (ρ), ignition mass flux at 50 kW/m^2 ($\dot{m}''_{ig}$), critical heat flux ($\dot{q}''_{B,crt}$) for near-limit blue flame, and extinction mass flux for yellow flame ($\dot{m}''_{ex,Y}$) and blue flame ($\dot{m}''_{ex,B}$) for different wood types, where the standard error of repeating tests is within 5%.

Wood sample	ρ (kg/m^3)	$\dot{m}''_{ig}$ (g/m^2·s)	$\dot{q}''_{B,crt}$ (kW/m^2)	$\dot{m}''_{ex,Y}$ (g/m^2·s)	$\dot{m}''_{ex,B}$ (g/m^2·s)
A	406	7.4	52	3.9	0.91
B	560	8.4	37	4.0	1.08
C	570	9.6	37	3.9	0.89
D	588	10.5	37	4.2	0.93
E	781	12.5	32	4.0	0.96
F	816	12.8	32	3.9	0.92

3. Experimental results

3.1. Fire processes and critical heat flux

Figure 3 shows the examples of fire phenomena of Wood C under different external radiation ($\dot{q}_e''$) of 30 kW/m^2 and 60 kW/m^2, respectively. The original videos can be found in Supplemental Materials (Video S1-2). The critical mass fluxes and time moments of transitioning to different stages are also indicated in Fig. 3. Before the piloted flaming ignition, smoke was always observed, likely the pyrolysis gases. Continuing the heating, a strong buoyancy-controlled yellow flame was piloted by the spark and maintained.

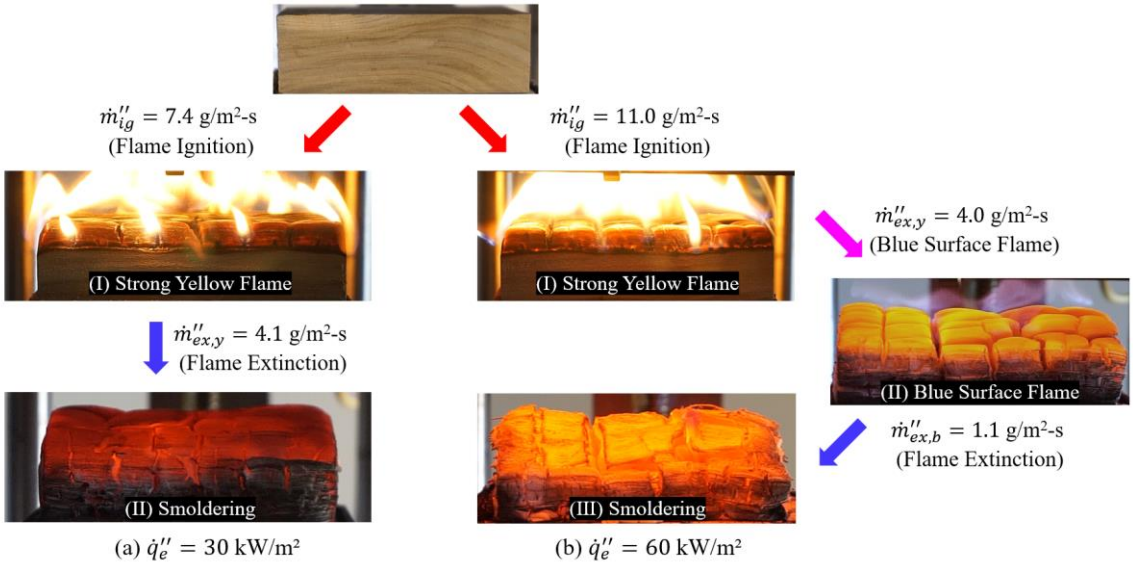

Fig. 3. Different burning of Wood C under irradiation ($\dot{q}_e''$) of (a) 30 kW/m^2, and (b) 60 kW/m^2.

Under the lower irradiation of 30 kW/m^2, a two-stage burning process was observed (Fig. 3a). After the extinction of the initial strong yellow flame, a stable smoldering fire in the solid phase occurred and sustained until burnout. On the other hand, under the higher irradiation of 60 kW/m^2, a three-stage burning process was observed (Fig. 3b). Specifically, after the extensive burning of yellow flame, a near-limit blue flame appeared and lasted for more than 20 min before transitioning to smoldering. This flame is weak, blue, flat, discrete above parts of the wood residue surface. The flame height is very small due to a small fuel mass flux (discussed more in Section 3.2), so the flame is only slightly affected by buoyancy effect. All of feathers are quite different from the regular yellow flame, as compared and summarized in Table 2. Note that the temperature of the observed blue flame is not necessarily lower than yellow flame, whereas it only indicate a lower soot concentration in the flame or soot standing away from hotter regions [34].

Fig. 4(a) compares the durations of strong yellow flame and near-limit blue flame of wood C as a function of external radiation, where the blue flame can last around 10 min longer than the yellow flame. The durations for both flame types decrease as the external irradiation increases, because the

external irradiation accelerates the burning processes. Moreover, the experiments have quantified the critical (minimum) irradiation level for the appearance of this near-limit blue flame ($\dot{q}_b''$) and the three-stage combustion processes. As showed in Table 1 and Fig. 4(b), the required critical heat flux is found to increase as wood density decreases, where the average value is about 40 ± 10 kW/m^2. Specifically, Wood F with the highest bulk density of 816 kg/m^3 can maintain the blue flame at the lowest critical irradiation of 32 kW/m^2, while the Wood A with the lowest density of 406 kg/m^3 requires the highest critical irradiation of 52 kW/m^2.

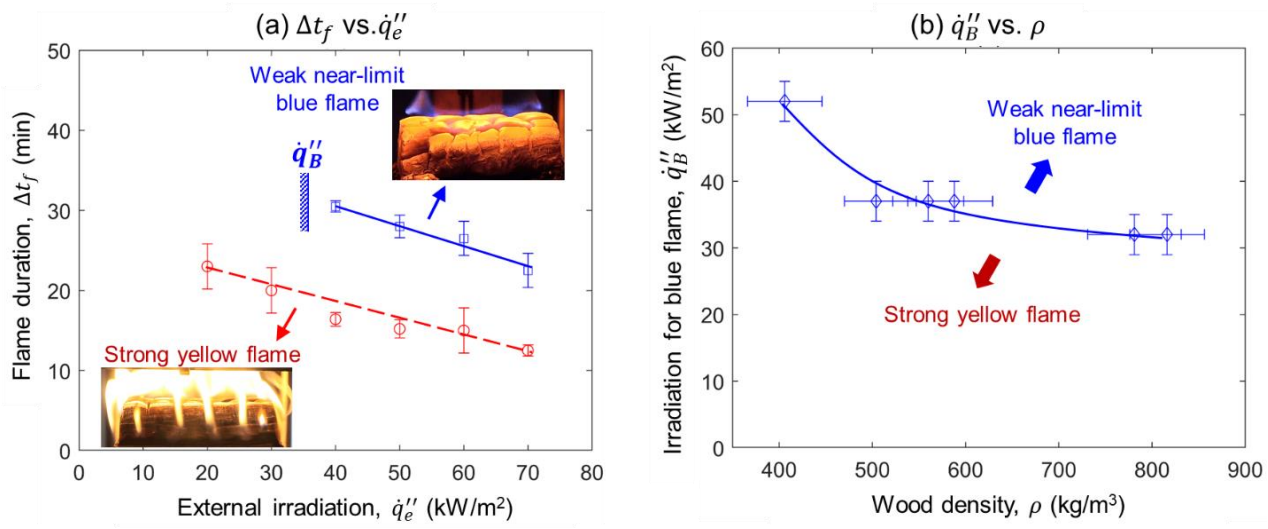

Fig. 4. (a) Durations of strong yellow flame and near-limit blue flame of wood C as a function of external irradiation, and (b) critical irradiation for blue flame vs. wood density, where the error bar shows the standard deviation of repeating tests.

Table 2. Phenomenological comparison between the near-limit blue flame and normal yellow flame.

Flame characteristics	Color	Intensity	Smoke	Continuity	Shape	Height	Buoyancy effect	Cover sample
Near-limit flame	blue	weak	invisible	discrete	flat	< 5 cm	weak	partial
Normal flame	yellow	strong	visible	continuous	conic	> 5 cm	strong	complete

In the real fire scenarios, wood materials may receive high irradiation from nearby hot smokes or flames (e.g., > 80 kW/m^2 in post-flashover compartment fires and wildland fires) [9]. Therefore, one can expect that after the disappearance of intense yellow flame, this kind of blue flame can still be sustained on timber for an extended period, although it may be too weak to be clearly visible. Also, as the blue flame does not entirely cover the wood surface, oxygen molecules may diffuse into the charred wood, so that smoldering may co-exist with the flame. Thus, this unique blue flame may not only help evaluate the fire risk of timber materials under real fire scenarios, but also play an essential role in the transition between flaming and smoldering.

3.2. Critical Mass flux

The mass flux ($\dot{m}''$) is the mass-loss rate (or burning rate) per unit area, which is considered as one of the most important parameters to quantify different forms of combustion [35]. During the flaming combustion, the increasing thickness of the char layer can reduce the amount of the heat the pyrolysis front receives like a thermal insulator, and extinction occurs when heating is too small to maintain the minimum mass flux ($\dot{m}''_{ex}$) [15,16]. Fig. 5 illustrates the evolution of mass flux of Wood C (570 kg/m^3) under external radiations of (a) 30 and (b) 60 kW/m^2, where CO/CO$_2$ ratio is also plotted for further comparison (See more subplots in Fig. A2 of Appendix).

At the lower irradiation of 30 kW/m^2 (Fig. 5a), the mass flux curve is similar to the typical evolution in [12]. Once exposed to the irradiation, the mass flux increases dramatically to a peak value, and then, it decreases gradually due to the build-up of the char layer on the top surface. Continuing the heating, the pyrolysis front gradually reaches the bottom of the wood sample and approaches to the top of the insulation board, so that the in-depth heat conduction into the wood is reduced. As a result, the pyrolysis is accelerated and results in the second peak of the mass loss curve. Afterward, the whole sample surface is mostly charred, and the mass flux goes through a sharp drop. Eventually, the self-extinction of the yellow flame occurs when the mass flux decreases to about 4 g/m^2·s. This value is consistent with previous studies on the critical mass flux for flaming extinction [9,15,36,37].

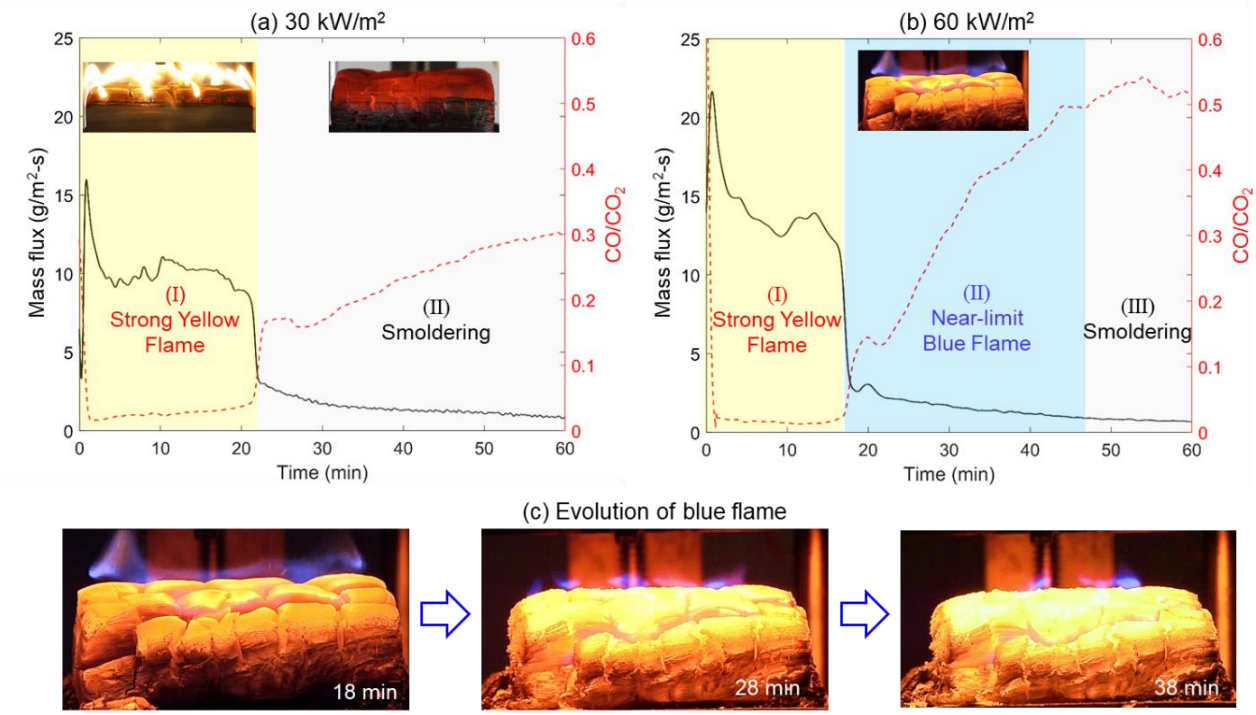

Fig. 5. Evolution of mass flux and CO/CO$_2$ ratio of Wood C under the external radiation ($\dot{q}''_e$) of (a) 30 kW/m^2, and (b) 60 kW/m^2; (c) evolution of blue flame above the wood surface.

On the other hand, under the higher irradiation of 60 kW/m^2, as shown in Fig. 5(b), extinction of the yellow flame also occurs when the mass flux decreases to about 4 g/m^2·s. Afterward, a blue flame closely attached to the sample surface occurs and maintains for more than 20 minutes at a lower mass flux (1~4 g/m^2·s), rather than directly transitioning to smoldering at 4 g/m^2·s. In this circumstance, the self-extinction of the flame should be the extinction of this blue flame, rather than the traditional buoyancy-controlled yellow flame. Therefore, the existence of this blue flame may extend the extinction limit of timber materials. As the mass flux decreases, the CO/CO_2 ratio continuously increases from 0.03 to 0.5. As one can see from Fig. 5c, as time goes by, the blue flame splits into discrete blue flamelets, reducing the area covered by flame so that more unburned CO may release to the ambient. Eventually, the near-limit blue flame extinguishes and transitions to smoldering at the critical (minimum) mass flux around $\dot{m}''_{ex} \approx 1$ g/m^2·s, re-defining the flame extinction limit of timber materials. During the smoldering stage, the CO/CO_2 ratio remains almost constant at about 0.5.

Fig. 6 further summarizes the true critical mass flux for the flame extinction ($\dot{m}''_{ex}$) under real fire scenarios with different external radiations, where the error bar shows the standard deviation of repeating tests. The critical mass fluxes for the piloted flaming ignition (8-14 g/m^2·s) are also presented, which is above the extinction limit. When the external radiation is lower than 40 kW/m^2, the yellow flame extinguishes at about 4 g/m^2·s, agreeing with the literatures [9,15]. When the external radiation is above 40 kW/m^2, the long-lasting blue flame can be sustained until $\dot{m}''_{ex} \approx 1$ g/m^2·s. Moreover, this redefined flame-extinction limit was found to be insensitive to the wood type, as shown in Table 1. This blue flame significantly reduces the minimum mass flux to sustain flaming wood combustion and extends the flame extinction limit, therefore suggesting that the blue flame combustion mode as well as the extinction mass flux measured herein should be considered in evaluating the fire risk of timber materials in the future.

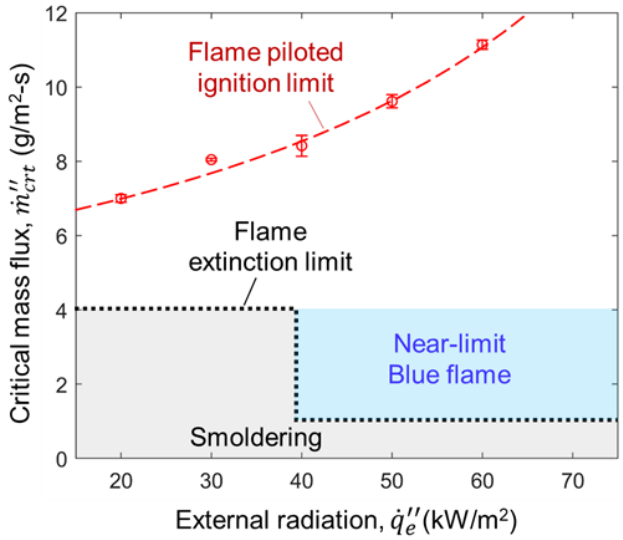

Fig. 6. The critical mass flux ($\dot{m}''$) as a function of the external radiation ($\dot{q}''_e$) for ignition, extinction, and different combustion phenomena of wood C.

3.3. Surface temperature

As the external radiation increases, the sample top-surface temperature (T_s) will increase as well. Fig. 7(a) shows the time evolution of the top surface temperature under 30 and 60 kW/m^2 of the same tests in Fig. 5(a-b) (see more examples in Fig. A3 of Appendix). Essentially, the top surface temperature approaches to the quasi-steady state by balancing the heat loss and, as expected, increases with the external radiation.

Fig. 7(b) further shows how the steady surface temperature varies with external radiation and affects the fire phenomena. It can be seen that the near-limit blue flame may survive only when the surface temperature is sufficiently high, that is, $T_s > T_B \approx 700$ ℃ at $\dot{q}_e'' > \dot{q}_B'' \approx 40$ kW/m^2. If the external radiation is lowered during the blue-flame region ($\dot{m}''$= 1-4 g/m^2·s), the surface temperature decreases to be lower than 700 ℃, and the blue flame eventually disappears. Once reapplying the irradiation, the blue flame will re-occur (see Video S3 in the Supplemental Materials). Thus, a hot enough surface temperature (maintained by a high external irradiation) may be a necessary condition for the occurrence of this blue flame (see more discussion in Section 3.4).

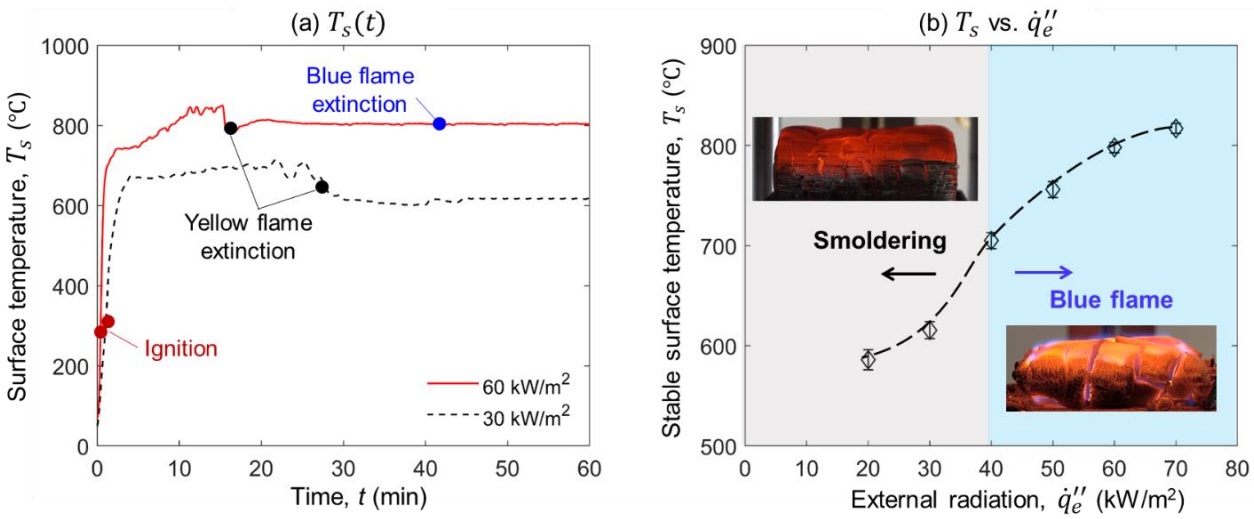

Fig. 7. (a) Time evolution of the top surface temperature under 30 and 60 kW/m^2, and (b) steady surface temperature (T_s) as a function of external radiation ($\dot{q}_e''$) of Wood C.

3.4. Phenomenological analysis

Considering the blue flame is never observed in PMMA regardless of the irradiation level, the decomposition chemistry and charring tendency of wood fuels are expected to play an important role in this near-limit flame behavior. To maintain a wood flame, at least two kinds of reactions are needed, namely, the pyrolysis of solid fuel to release pyrolyzates and the subsequent oxidation reaction of the pyrolyzates in the gas phase:

$$\text{Wood} \xrightarrow[\text{Flame/radiation}]{\text{External heating}} \text{Char} + \text{Pyrolyzates} \qquad \text{(Wood pyrolysis)} \qquad (1a)$$

$$\text{Pyrolyzates} + O_2 \rightarrow CO_2 + H_2O(g) \qquad \text{(Strong yellow flame)} \qquad (2)$$

Pyrolysis is maintained by the heating from flame and external irradiation, and a robust sooty yellow flame will persist until the pyrolysis is weakened by the thick char layer which is a good thermal insulator [38] (Fig. 8a). In contrast, for non-charring fuels like PMMA, there will always be a yellow flame until burnout (see Fig. A5). Compared to the low-temperature solid-phase oxidation, gas-phase flame reactions are much faster. Thus, almost all ambient oxygen will be consumed within the flame sheet, whereas little oxygen can diffuse into the porous char to sustain robust smoldering combustion.

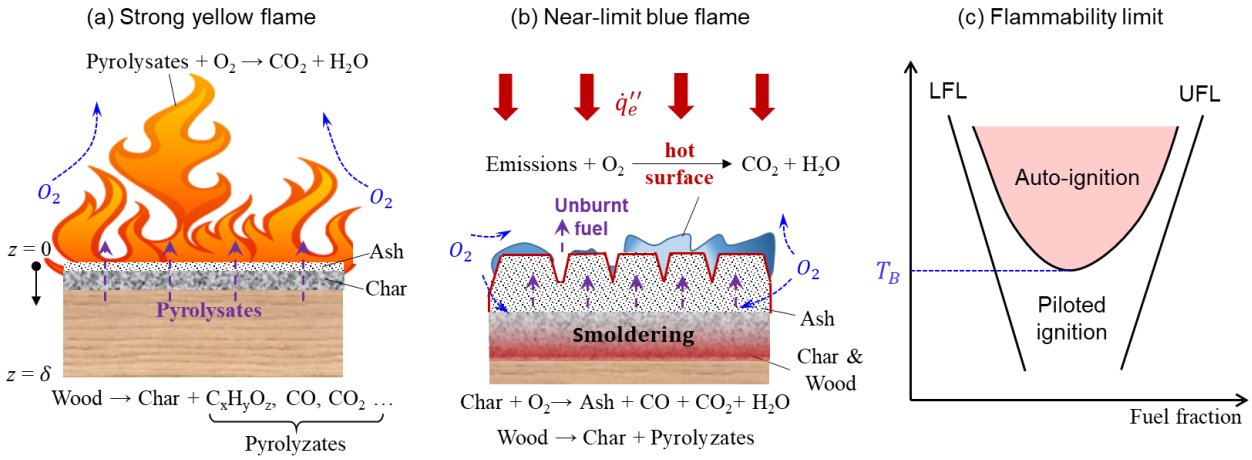

Fig. 8. Schematic diagrams of (a) strong yellow flame, (b) weak blue flame, and (c) the flammability limit for piloted and auto-ignition.

As the char layer builds up to weaken the effectiveness of the heating, less fuel is produced to support the flame. Under such a negative feedback, eventually, the yellow flame extinguishes at $\dot{m}''_{ex} \approx 4$ g/m^2·s, which may leave undecomposed wood in-depth and unburned char near the surface. Afterward, without the blockage of flame, oxygen may diffuse into the cracked and porous char layer to sustain smoldering combustion.

$$\text{Char} + O_2 \rightarrow \text{Ash} + C_xH_yO_z + CO + CO_2 + H_2O(g) \qquad \text{(Char oxidation)} \qquad (3)$$

This heterogeneous char oxidation is incomplete, which may produce a fuel mixture of hydrocarbons and CO [39,40], as also shown in the cone-calorimeter measurement (Fig. 5a-b). Moreover, the internal heat release from the char oxidation may further pyrolyze the wood in-depth as

$$\text{Wood} \xrightarrow[\text{Smoldering}]{\text{Internal heating}} \text{Char} + \text{Pyrolyzates} \qquad \text{(Wood pyrolysis)} \qquad (1b)$$

Especially, compared to the pyrolysis of the cellulose and hemicellulose components, the lignin component has not only a higher starting pyrolysis temperature (400-500 °C), but also a higher ending

pyrolysis temperature (>600 ℃) [41], as seen from the TG curves in Fig. A1(a). Thus, the lignin component may continue to pyrolyze and produce a small amount of flammable gas fuel before being oxidized to ash.

As the surface temperature increases with the external radiation, eventually, it may become hot enough (>700 ℃) to either pilot the flame or supports an auto-ignition of the fuel/air mixture. As illustrated in Fig. 8(b), it is hypothesized that the near-limit blue flame may be maintained by the mixture produced from both char-oxidation and in-depth wood-pyrolysis of smoldering processes

$$\text{Smoldering emission} + O_2 \xrightarrow{\text{hot surface}} CO_2 \qquad \text{(Near-limit blue flame)} \quad (4)$$

There are two pieces of supporting evidence, (1) the discrete blue flame partially covers the char may allow the oxygen diffusion inside to maintain the char oxidation that releases heat to sustain in-depth pyrolysis (mainly lignin), (2) the CO emission, as the sign of smoldering, in the blue-flame region in Fig. 5(b) (60 kW/m^2) is comparable to the pure smoldering region in Fig. 5(a) (30 kW/m^2), as part of the CO may be consumed by blue flame (CO/CO_2 ratio during smoldering process generally increases as external irradiation increases [25]).

The critical surface temperature of $T_B \approx 700$ ℃ to sustain the blue flame may be the minimum auto-ignition temperature (AIT) of the mixed hydrocarbons and CO produced from smoldering, as illustrated in Fig. 8(c). Below this temperature, the flammable mixture cannot be ignited without a pilot source. Above this temperature, the auto-ignition of the fuel-lean mixture not only ensures the existence of flame but also acts as a piloted source to ignite the nearby lean mixture. Because the release of smoldering emission is not uniform across the wood sample, the random ignition and flame propagation on the fuel surface makes the flame flicker around. In other words, this blue flame might be partially premixed. As the flame reaction takes place near the hot surface, and the fuel mass flux is small, the role of buoyancy may be too small to create a clear conical shape. Moreover, the color of a fuel-lean near-limit flame is pale blue because the low burning rates may result in small flames with small residence time, preventing aggolomeration of soot [42,43].

In short, two necessary conditions are hypothesized for this unique blue flame,

(I) The robust in-depth pyrolysis should be sustained by the internal smoldering combustion and external heating; and

(II) A hot surface temperature (>700 ℃) above the auto-ignition temperature of gaseous fuel should be maintained by the external radiation.

Further decreasing the fuel mass flux to about 1 g/m^2·s, the composition of the fuel-lean mixture near the hot surface may become lower than the lean flammability limit, giving rise to extinction. On the other hand, for non-charring fuels like PMMA, the surface temperature cannot reach 700 ℃, because pyrolysis reactions will be completed before exceeding 450 ℃, as shown in Figs. A1(b) and A5(b).

Note that the critical values presented in the work are bounded to the experimental conditions,

e.g., the irradiation from the cone, and material properties (e.g., types of timber, sample sizes and preparations). To further explain the combustion mechanism responsible for the near-limit blue flame and verify the aforementioned two hypotheses, the future research could establish two different numerical models to decouple this complex problem. First, a solid-phase model is constructed to demonstrate the necessity of smoldering combustion (or char oxidation) in maintaining the pyrolysis reaction and a long-lasting fuel mass flux of 1~4 g/m^2·s after the extinction of strong yellow flame. Then, a gas-phase DNS model can be constructed to demonstrate the necessity of a hot surface and a critical mass flux to main a near-limit flame that is rarely affected by buoyancy.

4. Conclusions

In this study, a unique wood combustion mode showing a near-limit blue flame was identified as an intermediate combustion mode between the buoyancy-controlled yellow flame and the smoldering combustion. The blue flame may appear only if the external radiation exceeds a critical value of about 40 kW/m^2 and the surface temperature higher than 700℃. This near-limit flame tends to attach to the hot charring and smoldering surface and may be only affected by buoyancy effect slightly. Below the critical irradiation, the intense yellow flame directly transitions to smoldering when the mass flux decreases to about 4.0 g/m^2·s for all wood samples. Above the critical irradiation, on the other hand, the near-limit blue flame may still survive until the mass flux of 1.0 g/m^2·s. Thus, it may redefine the flame extinction limit of timber materials under external radiation.

This work proposes two necessary conditions for the occurrence of near-limit blue flame, (I) in-depth pyrolysis sustained by the internal smoldering combustion, and (II) the hot surface maintained by large external radiation to extend the flammability limit or achieve autoignition. The future work will focus on emission gas compositions from different combustion stages, as well as numerical simulations coupling gas-phase and solid-phase processes. This unique blue flame may play an essential role in the transition between flaming and smoldering and help evaluate the fire risk of timber materials under real fire scenarios.

References

[1] Barber D. Tall Timber Buildings: What's Next in Fire Safety? *Fire Technology* 2015;51:1279–84.

[2] Richter F, Atreya A, Kotsovinos P, Rein G. The effect of chemical composition on the charring of wood across scales. *Proceedings of the Combustion Institute* 2019;37:4053–61.

[3] Richter F, Kotsovinos P, Rackauskaite E, Rein G. Thermal Response of Timber Slabs Exposed to Travelling Fires and Traditional Design Fires. *Fire Technology* 2020.

[4] Crielaard R, van de Kuilen JW, Terwel K, Ravenshorst G, Steenbakkers P. Self-extinguishment of cross-laminated timber. *Fire Safety Journal* 2019;105:244–60.

[5] Song J, Chen C, Zhu S, Zhu M, Dai J, Ray U, et al. Processing bulk natural wood into a high-

performance structural material. *Nature* 2018;554:224–8.

[6] Boarin P, Calzolari M, Davoli P. Two timber construction models: tradition without innovation or innovation without tradition? 2018.

[7] Drysdale D. An Introduction to Fire Dynamics. 3rd ed. Chichester, UK: John Wiley & Sons, Ltd; 2011.

[8] Prior R. The entire wooden interior of Notre Dame Cathedral has been lost. *CNN* 2019.

[9] Emberley R, Inghelbrecht A, Yu Z, Torero JL. Self-extinction of timber. *Proceedings of the Combustion Institute* 2017;36:3055–62.

[10] Bilbao R, Mastral JF, Aldea ME, Ceamanos J, Betrán M, Lana JA. Experimental and theoretical study of the ignition and smoldering of wood including convective effects. *Combustion and Flame* 2001;126:1363–72.

[11] Bartlett AI, Hadden RM, Bisby LA. A Review of Factors Affecting the Burning Behaviour of Wood for Application to Tall Timber Construction. *Fire Technology* 2019;55:1–49.

[12] Boonmee N, Quintiere JG. Glowing and flaming autoignition of wood. *Proceedings of the Combustion Institute* 2002;29:289–96.

[13] Boonmee N, Quintiere JG. Glowing ignition of wood: The onset of surface combustion. *Proceedings of the Combustion Institute* 2005;30 II:2303–10.

[14] Richter F, Atreya A, Kotsovinos P, Rein G. The effect of chemical composition on the charring of wood across scales. *Proceedings of the Combustion Institute* 2017;000:1–9.

[15] Emberley R, Do T, Yim J, Torero JL. Critical heat flux and mass loss rate for extinction of flaming combustion of timber. *Fire Safety Journal* 2017;91:252–8.

[16] Moghtaderi B, Novozhilov V, Fletcher DF, Kent JH. A New Correlation for Bench-scale Piloted Ignition Data of Wood. *Fire Safety Journal* 1997;29:41–59.

[17] Vermesi I, Richter F, Chaos M, Rein G. Ignition and Burning of Fibreboard Exposed to Transient Irradiation. *Fire Technology* 2020.

[18] Shi L, Chew MYL. Influence of moisture on autoignition of woods in cone calorimeter. *Journal of Fire Sciences* 2012;30:158–69.

[19] Huang X, Li K, Zhang H. Modelling bench-scale fire on engineered wood: Effects of transient flame and physicochemical properties. *Proceedings of the Combustion Institute* 2017;36:3167–75.

[20] Richter F, Rein G. Heterogeneous kinetics of timber charring at the microscale. *Journal of Analytical and Applied Pyrolysis* 2019;138:1–9.

[21] Richter F, Rein G. A multiscale model of wood pyrolysis to study the role of chemistry and heat transfer at the mesoscale. *Combustion and Flame* 2020;216:316–25.

[22] Rein G. Smoldering Combustion. *SFPE Handbook of Fire Protection Engineering* 2014;2014:581–603.

[23] Gratkowski MT, Dembsey NA, Beyler CL. Radiant smoldering ignition of plywood. *Fire*

Safety Journal 2006;41:427–43.

[24] Wang S, Ding P, Lin S, Huang X, Usmani A. Deformation of wood slice in fire: Interactions between heterogeneous chemistry and thermomechanical stress. *Proceedings of the Combustion Institute* 2021;38:5081–90.

[25] Lin S, Sun P, Huang X. Can peat soil support a flaming wildfire? *International Journal of Wildland Fire* 2019;28:601–13.

[26] Bartlett AI, Hadden RM, Hidalgo JP, Santamaria S, Wiesner F, Bisby LA, et al. Auto-extinction of engineered timber: Application to compartment fires with exposed timber surfaces. *Fire Safety Journal* 2017;91:407–13.

[27] Richter F, Jervis FX, Huang X, Rein G. Burning rate of wood pyrolysis, smouldering, and flaming: Effect of oxygen. *Combustion and Flame (under Review)* 2020.

[28] Cuevas J, Torero JL, Maluk C. Flame extinction and burning behaviour of timber under varied oxygen concentrations. *Fire Safety Journal* 2020:103087.

[29] Arnórsson SM, Hadden RM, Law A. The Variability of Critical Mass Loss Rate at Auto-Extinction. *Fire Technology* 2020.

[30] Babrauskas V. Journal of Fire Protection Ignition of Wood : A Review of the State of the Art. *Journal of Fire Protection Engineering* 2002;12:163–89.

[31] Smucker BD, Mulky TC, Cowan DA, Niemeyer KE, Blunck DL. Effects of fuel content and density on the smoldering characteristics of cellulose and hemicellulose. *Proceedings of the Combustion Institute* 2019;37:4107–16.

[32] Santoso MA, Christensen EG, Yang J, Rein G. Review of the Transition From Smouldering to Flaming Combustion in Wildfires. *Frontiers in Mechanical Engineering* 2019;5.

[33] Babrauskas V. The Cone Calorimeter. In: Hurley M, editor. SFPE Handb Fire Prot Eng. 5th Editio, London: Springer; 2016, p. 952–80.

[34] Fuentes A, Legros G, Claverie A, Joulain P, Vantelon JP, Torero JL. Interactions between soot and CH* in a laminar boundary layer type diffusion flame in microgravity. *Proceedings of the Combustion Institute* 2007;31 II:2685–92.

[35] Rich D, Lautenberger C, Torero JL, Quintiere JG, Fernandez-Pello C. Mass flux of combustible solids at piloted ignition. *Proceedings of the Combustion Institute* 2007;31 II:2653–60.

[36] Delichatsios MA, Delichatsios MM. Critical Mass Pyrolysis Rates for Extinction of Fires over Solid Materials n.d.:153–64.

[37] Delichatsios MA. Piloted ignition times, critical heat fluxes and mass loss rates at reduced oxygen atmospheres. *Fire Safety Journal* 2005;40:197–212.

[38] Moghtaderi B, Novozhilov V, Fletcher DF, Kent JH. A New Correlation for Bench-scale Piloted Ignition Data of Wood. *Fire Safety Journal* 2006;29:41–59.

[39] Rein G, Cohen S, Simeoni A. Carbon emissions from smouldering peat in shallow and strong

fronts. *Proceedings of the Combustion Institute* 2009;32:2489–96.

[40] Wu D, Schmidt M, Huang X, Verplaetsen F. Self-ignition and smoldering characteristics of coal dust accumulations in O2/N2 and O2/CO2 atmospheres. *Proceedings of the Combustion Institute* 2017;36:3195–202.

[41] Stefanidis SD, Kalogiannis KG, Iliopoulou EF, Michailof CM, Pilavachi PA, Lappas AA. A study of lignocellulosic biomass pyrolysis via the pyrolysis of cellulose, hemicellulose and lignin. *Journal of Analytical and Applied Pyrolysis* 2014;105:143–50.

[42] Lin K-C, Faeth GM. State Relationships of Laminar Permanently-Blue Opposed-Jet Hydrocarbon-Fueled Diffusion Flames. *Int J Environ Combust Tech Vol I* 2000:53–79.

[43] Lin KC, Faeth GM. Hydrodynamic suppression of soot emissions in laminar diffusion flames. *33rd Aerospace Sciences Meeting and Exhibit* 1995;12:10–7.

Appendix

The wood and pmma sample were pulverized into powders and dried at 70 °C for 48 h. The thermal analysis was conducted with a PerkinElmer STA 6000 Simultaneous Thermal Analyzer. The initial mass was about 3 mg, and samples were heated at the constant rates of 30 K/min. Two oxygen concentrations were selected, 0% (nitrogen) and 21% (air), with a flow rate of 50 mL/min. Experiments were repeated twice for each case, and good repeatability is shown. As compared in Fig. A1, the decomposition both started at more than 200 °C, while the DTG curve of wood is much wider than that of PMMA. Clearly, the reaction of PMMA already finished right below 500 °C. For the DTG curve of wood, the decomposition of wood (especialy the lignin component) can still exist above 600 °C.

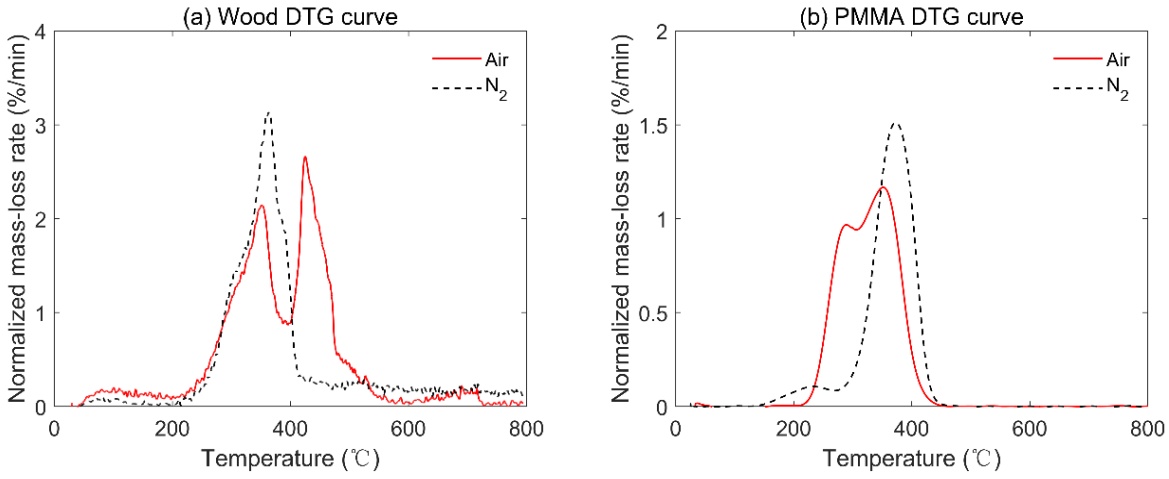

Fig. A1. TGA results of (a) wood C and (b) PMMA under air and nitrogen flow at a heating rate of 30 K/min.

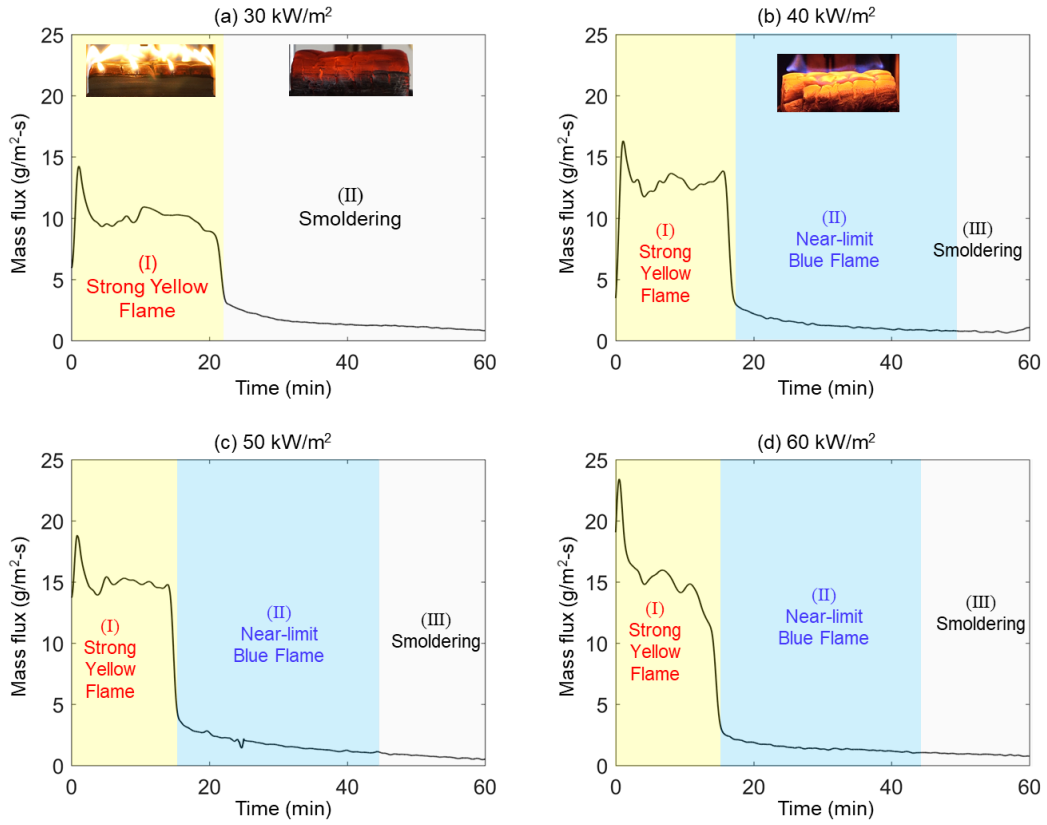

Fig. A2. Evolution of mass flux of Wood C under the external radiation ($\dot{q}_e''$) of (a) 30 kW/m^2, (b) 40 kW/m^2, (c) 50 kW/m^2, and (d) 60 kW/m^2.

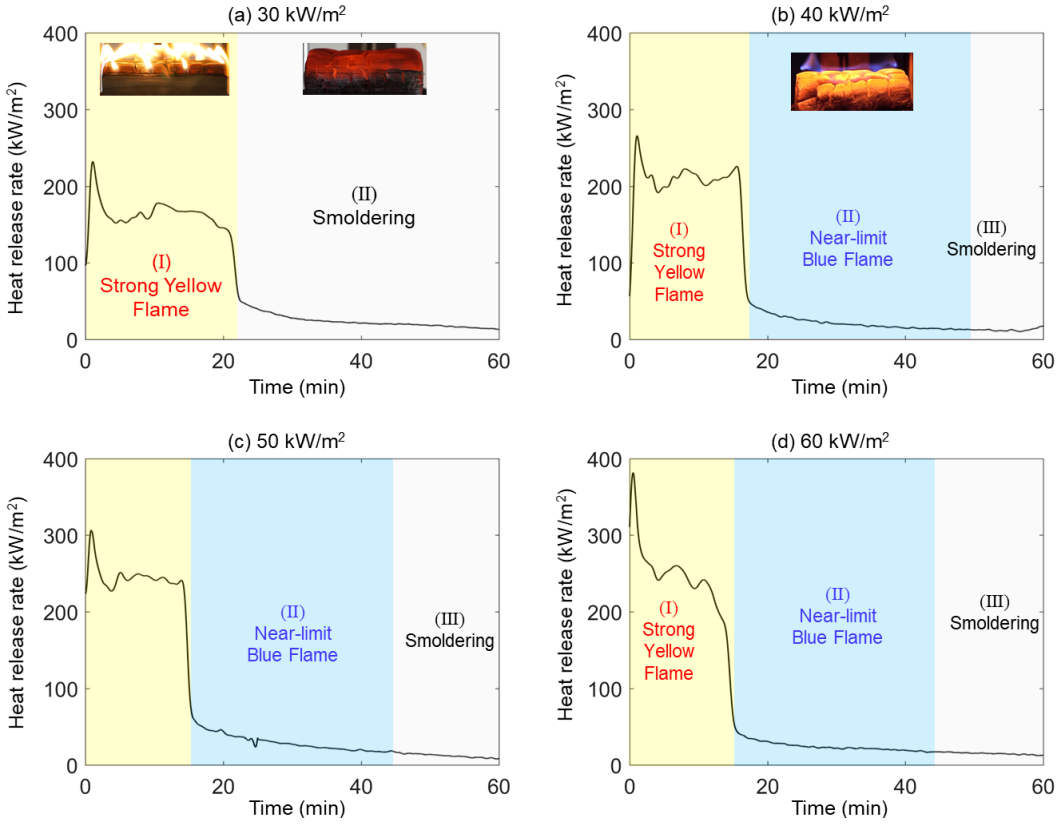

Fig. A3. Evolution of heat release rate of Wood C under the external radiation ($\dot{q}_e''$) of (a) 30 kW/m^2, (b) 40 kW/m^2, (c) 50 kW/m^2, and (d) 60 kW/m^2.

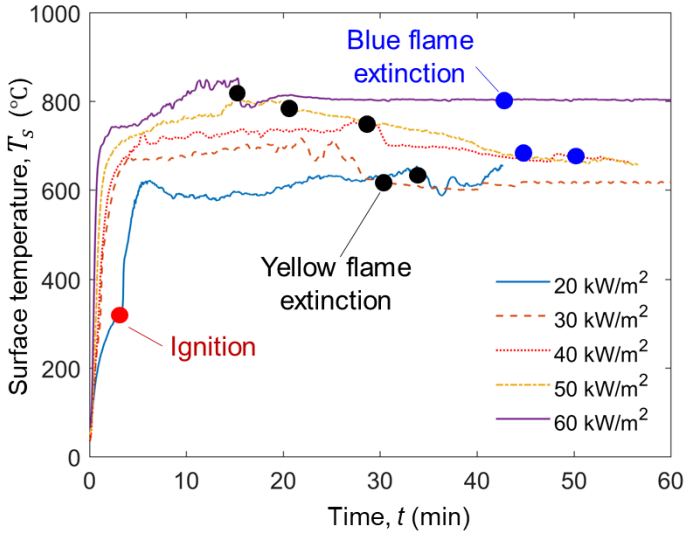

Fig. A4. Time evolution of the top surface temperature under external heat flux from 20 to 60 kW/m^2.

Fig. A5 shows the mass flux and temperature evolution of PMMA under the external radiant heat flux of 60 kW/m^2. The mass flux evolution of PMMA is different from that of wood in Fig. 5. For PMMA, the mass flux approximately sustained at 20 g/m^2-s during burning, and the extinction occurred due to the burnout of fuel. In Fig. A5(b), during the flaming combustion, the top surface temperature was measured to be constant at about 400 °C before the burnout. The value is also close to final temperature of DTG in Fig. A1(b).

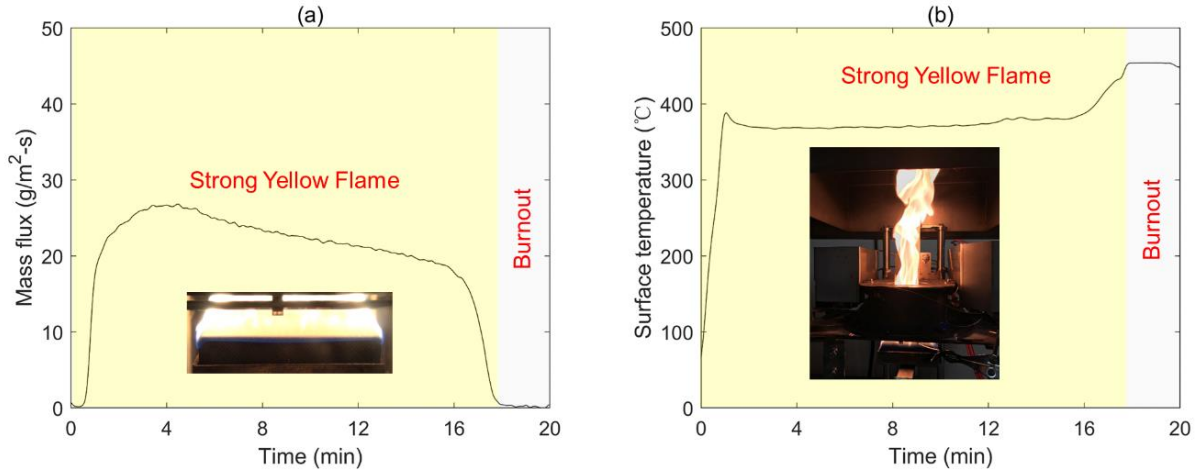

Fig. A5. The mass flux evolution and surface temperature of PMMA under the external radiation of 60 kW/m^2.